ELSEVIER

Electrochemistry Communications 4 (2002) 989–994

electrochemistry communications

www.elsevier.com/locate/elecom

Preparation and characterization of nano-crystalline $LiNi_{0.5}Mn_{1.5}O_4$ for 5 V cathode material by composite carbonate process

Y.S. Lee [a], Y.K. Sun [b], S. Ota [c], T. Miyashita [c], M. Yoshio [a,*]

[a] *Department of Applied Chemistry, Saga University, 1 Honjo, Saga 840-8502, Japan*
[b] *Department of Chemical Engineering, Hanyang University, 17 Haengdang-dong, Seoul 133-791, South Korea*
[c] *Chuo-denki Kogyo, 272 Taguchi, Myokokogen, Nakakubiki, Niigata 949-2193, Japan*

Received 27 August 2002; accepted 4 October 2002

Abstract

$LiNi_{0.5}Mn_{1.5}O_4$ has been synthesized using two different synthetic methods; a sol–gel method and a composite carbonate process. $LiNi_{0.5}Mn_{1.5}O_4$ obtained by the sol–gel method showed a nickel oxide impurity in the XRD diagram and two voltage plateaus at 4.1 and 4.7 V upon cycling. However, the $LiNi_{0.5}Mn_{1.5}O_4$ compound obtained by the composite carbonate process exhibited a pure cubic spinel structure ($Fd\bar{3}$ m) without any impurities and only one voltage plateau at 4.7 V in the charge/discharge curves. Furthermore, it showed an excellent cycling retention rate of over 96% in the high temperature test. The well-developed $LiNi_{0.5}Mn_{1.5}O_4$ obtained by the composite carbonate process contained many spherical particles of about 3–4 μm, made up of small nano-sized particles (50–100 nm). It was a unique powder characterization and these nano-sized particles improved the cycling performance of the $LiNi_{0.5}Mn_{1.5}O_4$ obtained by composite carbonate process.

Keywords: Spinel; $LiNi_{0.5}Mn_{1.5}O_4$; Voltage plateau; Nano-sized; Lithium batteries

1. Introduction

Layered lithium metal oxide and spinel lithium manganese oxide have been selected as the preferred cathode materials for lithium secondary batteries [1–10]. Layered lithium metal oxide with the general formula $LiMO_2$ (M = Co, Ni, Mn) has a rock salt structure where lithium and a transition metal cation occupy alternate layers of octahedral sites in a distorted close-packed oxygen ion lattice. Newly designed lithium cathode materials, such as $Li[Ni_xLi_{(1/3-2x/3)}Mn_{(2/3-x/3)}]O_2$ and $LiCo_{1/4}Ni_{3/4}O_2$, were recently reported for the next generation cathode material of lithium secondary batteries [3,4]. These materials exhibited a larger capacity and well-optimized charge/discharge plateaus, but they still required an improved cycling performance and thermal stability for the mid/large-scale batteries.

Although the reversible specific capacity for the spinel manganese oxide ($LiMn_2O_4$) is lower than the theoretical specific capacity of the lithium cobalt and nickel compounds, it potentially represents the most stable and the least expensive of the available cathode materials. In view of this point, the metal-ion doped spinel as a 5 V cathode material, $LiM_xMn_{2-x}O_4$ (M = Ni, Cr, Cu,...), was still an attractive and prospective cathode material for use in zero emission vehicles (ZEV), which needed a high energy density and good cycle stability [5–11]. Furthermore, Dahn and co-workers [7] recently suggested that all metal-doped spinels should be reinvestigated for the reversible deintercalation degree of lithium in the high voltage region (over 4.7 V). The role of the doped metal ions in the $Li/LiM_xMn_{2-x}O_4$ cell is to compensate for the capacity loss which originates from the oxidation of Mn^{3+} to Mn^{4+} below 4.5 V by oxidizing M^{2+} to M^{4+} (especially, M = Ni) over 4.5 V. This is the reason why the metal-doped spinel could maintain a high discharge capacity even when it operates in the high voltage region [7,11].

In general, $LiM_xMn_{2-x}O_4$ material was prepared by a conventional solid-state method at low (600–700 °C) or

* Corresponding author. Fax: +81-952-28-8673, +81-45-508-7480.
E-mail addresses: saga98ts32@yahoo.co.jp (Y.S. Lee), yoshio@ccs.ce.saga-u.ac.jp (M. Yoshio).

1388-2481/02/$ - see front matter © 2002 Elsevier Science B.V. All rights reserved.
PII: S1388-2481(02)00491-5

high temperature (750–850 °C) [12–14]. However, it involves many disadvantages such as inhomogeneity, irregular morphology, and larger particle sizes with a broader particle size distribution. In order to achieve the efficient lithium utilization at a high current density in the high voltage region, it is very necessary to obtain submicron-sized particles with a uniform morphology, narrow size distribution, and homogeneity.

Therefore, considerable improvements in the synthesis of high performance cathode materials have been accomplished by the wet method. Because the sol–gel method, which a kind of wet method, can produce highly homogeneous submicron-sized particles with a narrow particle size distribution, it significantly enhances the cycling performance of the electrode [15–17]. However, the sol–gel method also has some disadvantages such as a complex synthesis route and high synthetic cost, which is about three times that of the conventional solid-state method. It is also well known that $LiNi_{0.5}Mn_{1.5}O_4$ material as a 5 V cathode material is very difficult to obtain as a pure crystalline compound with the desired electrochemical properties, although it was synthesized using the wet method [17,18].

Therefore, we introduced a new synthetic method, the composite carbonate process, to be obtained a pure $LiNi_{0.5}Mn_{1.5}O_4$ powder for this study. This method, a new concept of combining the sol–gel and solid-state reactions, shared many advantages of the above two synthetic methods. The main advantage of the carbonate process is obtaining a well-developed stoichiometric $LiNi_{0.5}Mn_{1.5}O_4$ material with a higher surface area at a lower synthesis temperature (700 °C).

We report here that characteristics of the $LiNi_{0.5}Mn_{1.5}O_4$ for 5 V cathode material using the composite carbonate process and show the excellent cycling performance of this material both at room and high temperatures.

2. Experimental

To compare the effect of synthesis method, two $LiNi_{0.5}Mn_{1.5}O_4$ powders were synthesized by the sol–gel method and composite carbonate process. One $LiNi_{0.5}Mn_{1.5}O_4$ powder was synthesized using $Li(CH_3COO)\cdot H_2O$, $Ni(CH_3COO)\cdot 4H_2O$, and $Mn(CH_3COO)\cdot 4H_2O$ by the sol–gel method. Adiphic acid was used as the chelating agent in this study. The synthetic procedure for the sol–gel method has been as detailed elsewhere [16,17]. The other $LiNi_{0.5}Mn_{1.5}O_4$ powder was synthesized using $LiOH\cdot H_2O$, $NiSO_4$, $MnSO_4$, and $(NH_4)_2CO_3$ by the composite carbonate process. The stoichiometric amounts of nickel and manganese (1:3) were dissolved together in distilled water in beaker A (Solution A). The proper amount of ammonium carbonate was also dissolved in distilled water in beaker B (Solution B). Each solution was slowly poured into another beaker (Solution A + B) with heating at 80 °C until sediment formed. The obtained ($(Ni_{0.25}Mn_{0.75})CO_3$) complex after washing and drying was calcined at 600 °C for 48 h in air. After calcination, a stoichiometric amount of lithium was mixed with the ($Ni_{0.25}Mn_{0.75}$) complex and calcined again at 450 °C for 10 h in a box furnace. The final $LiNi_{0.5}Mn_{1.5}O_4$ powder was obtained after the last calcination for 24 h at 700 °C in air.

The powder X-ray diffraction (XRD, Rint 1000, Rigaku, Japan) using CuKα radiation was employed to identify the crystalline phase of the synthesized material. The contents of Li, Ni, and Mn in the resulting material were analyzed with an inductively coupled plasma spectrometer (ICP, SPS 7800, Seiko Instruments, Japan). The particle morphology of the $LiNi_{0.5}Mn_{1.5}O_4$ powder was observed using a scanning electron microscope (SEM, S-4000, Hitachi, Japan). The specific surface area of this powder was measured in a Gemini 2375 instrument by the Brunauer, Emmett, and Teller (BET) method.

The electrochemical characterizations were performed using CR2032 coin-type cell. The cathode was fabricated with 20 mg of accurately weighed active material and 12 mg of conductive binder (8 mg of Teflonized acetylene black (TAB) and 4 mg of graphite). It was pressed on 200 mm^2 stainless steel mesh used as the current collector under a pressure of 300 kg/cm^2 and dried at 180 °C for 5 h in an oven. The test cell was made of a cathode and a lithium metal anode (Cyprus Foote Mineral) separated by a porous polypropylene film (Celgard 3401). The electrolyte used was a mixture of 1 M $LiPF_6$-ethylene carbonate (EC)/dimethyl carbonate (DMC) (1:2 by vol., Ube Chemicals, Japan). The charge and discharge current density was 0.4 mA/cm^2 with a cut-off voltage of 3.5–5.2 V at room (25 °C) and high (50 °C) temperatures.

3. Results and discussion

Each property and the chemical analysis data of the two $LiNi_{0.5}Mn_{1.5}O_4$ powders synthesized by different synthetic methods, i.e., the sol–gel and complex carbonate methods, are shown in Table 1. It shows that the two powders are almost the same, which have the typical properties of $LiNi_{0.5}Mn_{1.5}O_4$, except for the difference in the surface area of the powders as a result of the different average particle size. This unique relation between surface area and particle size of two materials will be discussed in a subsequent section of this report.

Fig. 1 shows the X-ray diffraction patterns (XRD) of the $LiNi_{0.5}Mn_{1.5}O_4$ materials prepared using the two different synthetic methods. Although the two materials exhibited very similar physicochemical properties as shown in Table 1, the XRD patterns of these two

Table 1
Properties and chemical analysis data of $LiNi_{0.5}Mn_{1.5}O_4$

$LiNi_{0.5}Mn_{1.5}O_4$	Li (wt%)	Ni (wt%)	Mn (wt%)	Lattice constant (Å)	Ave. particle size (D_{50}, μm)	Surface area (m^2/g)
Sol–gel method (750 °C)	3.7	15.2	44.3	8.17	1.49	0.85
Carbonate process (700 °C)	3.7	15.4	44.8	8.19	3.46	3.71

materials are quite different. $LiNi_{0.5}Mn_{1.5}O_4$ obtained by the composite complex carbonate method (herein referred to as C-$LiNi_{0.5}Mn_{1.5}O_4$, Fig. 1(b)) showed a well-defined cubic spinel structure ($Fd\bar{3}$ m) without any impurities over the full scan range. However, $LiNi_{0.5}Mn_{1.5}O_4$ obtained by the sol–gel method (herein referred to as S-$LiNi_{0.5}Mn_{1.5}O_4$) displayed small amounts of impurities and a different intensity ratio of the (3 1 1)/(4 0 0) peaks. The main difference of these two materials was the presence/absence of impurities of $2\theta = 37.5°$, 43.8°, and 63.8°, which are the impurities of nickel oxide.

It is well known that $LiNi_{0.5}Mn_{1.5}O_4$ made by the solid-state method is very difficult to obtain as a pure spinel phase without any impurities [7,8]. Even though the same material is obtained by the sol–gel method, some research groups (including our group) failed to get a homogeneous $LiNi_{0.5}Mn_{1.5}O_4$ phase and to obtain the electrochemical characteristics peculiar to $LiNi_{0.5}Mn_{1.5}O_4$ [17,19,20]. We previously reported that $LiNi_xMn_{2-x}O_4$ obtained by the sol–gel method contained a NiO impurity when the nickel content was over 4.7 at 750 °C [17]. Dahn and co-workers [7] also reported that the formation of the $Li_{0.2}Ni_{0.8}O$ peak that resulted from the nickel deficiency in the $LiNi_xMn_{2-x}O_4$ structure. This means that even if a stoichiometric amount of nickel is used in the synthetic process (both solid-state and sol–gel method), extra amounts of nickel remained in the $LiNi_{0.5}Mn_{1.5}O_4$ powder and could not form a perfect solid solution in the $LiNi_{0.5}Mn_{1.5}O_4$ structure. This possibly results in the impurity of NiO or $Li_{0.2}Ni_{0.8}O$ in the XRD diagram.

From the previous reports, the $Li/LiNi_xMn_{2-x}O_4$ cell ($0 < x < 0.5$) had two distinct plateaus at 4.1 and 4.7 V in the charge/discharge curves during the cycling test. Also, it is well known that the 4.1 V plateau resulted from the oxidation of Mn^{3+} to Mn^{4+} and the 4.7 V one is the oxidation of Ni^{2+} to Ni^{4+}. When the doped nickel content of $LiNi_xMn_{2-x}O_4$ increases, the 4.1 V plateau gradually decreases, which due to the less energetic oxidation reaction from Mn^{3+} to Mn^{4+} because of the decreased amount of Mn^{3+} in the $LiNi_xMn_{2-x}O_4$ material. Because the oxidation states of Ni and Mn in the $LiNi_{0.5}Mn_{1.5}O_4$ were 2+ and 4+, which were already reported by Amine et al. [8] using XPS, respectively, a $Li/LiNi_{0.5}Mn_{1.5}O_4$ cell could display the only 4.7 V plateau of oxidation from Ni^{2+} to Ni^{4+} without concrete 4.1 V plateau in the charge/discharge curves. The reason for the increased voltage step from 4.1 to 4.7 V was due to the difference in the binding energy between Mn 3d e_g and Ni 3d e_g (about 0.5 eV) [7].

The charge/discharge curves of the $Li/LiNi_{0.5}Mn_{1.5}O_4$ cells obtained using the different synthetic methods are shown in Fig. 2. The first charge of the Li/S-$LiNi_{0.5}Mn_{1.5}O_4$ cell still showed a small 4.1 V plateau

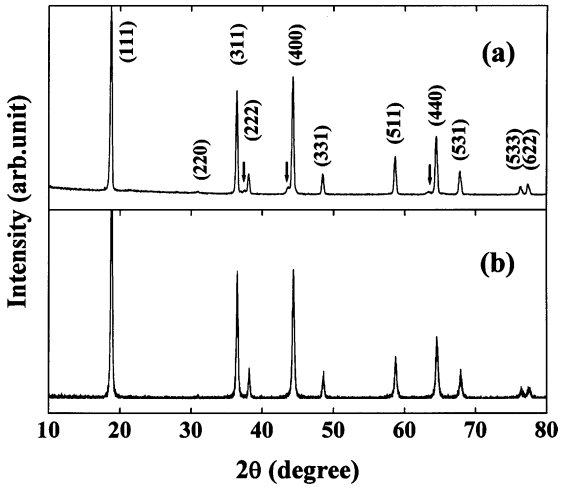

Fig. 1. X-ray diffraction (XRD) patterns of $LiNi_{0.5}Mn_{1.5}O_4$ obtained by the (a) sol–gel method and (b) composite carbonate process.

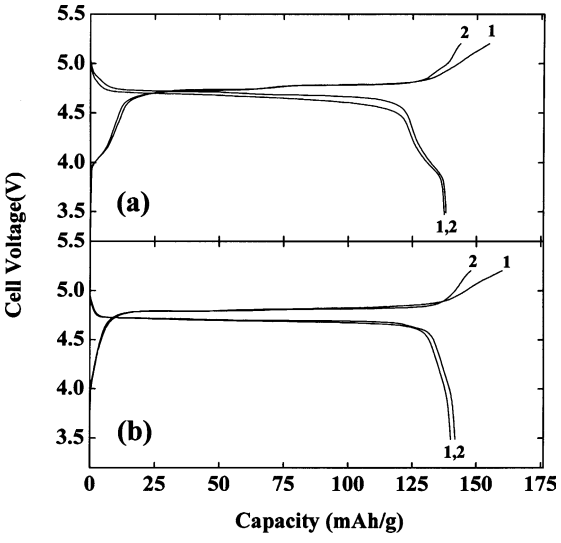

Fig. 2. The charge/discharge curves for the Li/1 M $LiPF_6$-EC/DMC/$LiNi_{0.5}Mn_{1.5}O_4$ obtained by the (a) sol–gel method and (b) composite carbonate process. The test condition was a current density of 0.4 mA/cm^2 between 5.2 and 3.5 V at room temperature.

and a concrete 4.7 V plateau (Fig. 2(a)). This indication appeared again in the next charge/discharge curves. This means that this cell underwent an oxidation reaction of Mn^{3+} to Mn^{4+} which resulted in the 4.1 V plateau during cycling as mentioned above. It could be a proof that doped nickel ions of $LiNi_{0.5}Mn_{1.5}O_4$ obtained by the sol–gel method in this study failed to perfectly substitute into the $LiMn_2O_4$ spinel structure. While the Li/C-$LiNi_{0.5}Mn_{1.5}O_4$ cell showed only one clear voltage plateau at 4.7 V, this voltage shape was still maintained after the 50th cycle. Based on these results, we found that $LiNi_{0.5}Mn_{1.5}O_4$ obtained by the composite carbonate process was successfully synthesized and exhibited the typical characteristics of a $Li/LiNi_{0.5}Mn_{1.5}O_4$ cell.

Fig. 3 shows the variation in the specific discharge capacity with the number of cycles for the $LiNi_{0.5}Mn_{1.5}O_4$ materials obtained by the different methods. The charge/discharge current density was 0.4 mA/cm^2 with a cut-off voltage of 3.5–5.2 V at room and high temperatures. The two $LiNi_{0.5}Mn_{1.5}O_4$ compounds showed a very stable cycling behavior at room temperature and the cycling retention rate after 50 cycles was over 97%. However, the two materials showed a quite different cycle behavior in the high temperature test. C-$LiNi_{0.5}Mn_{1.5}O_4$ also showed an excellent cycling performance at high temperature, although the last discharge capacity was slightly decreased. On the other hand, S-$LiNi_{0.5}Mn_{1.5}O_4$ presented a very poor cycling performance with a cycle retention rate of 34%.

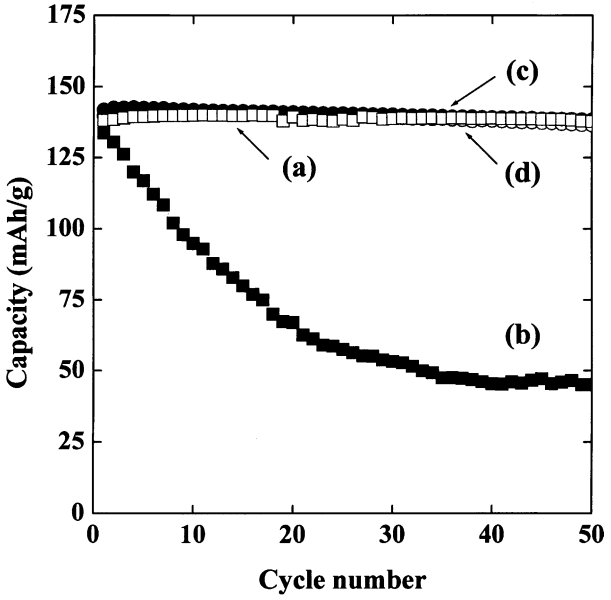

Fig. 3. Plots of the specific discharge vs. number of cycles for the Li/1 M $LiPF_6$-EC/DMC/$LiNi_{0.5}Mn_{1.5}O_4$ obtained by the sol–gel method ((a) 25 °C, (b) 50 °C)) and composite carbonate process ((c) 25 °C, (d) 50 °C)). The test condition was a current density of 0.4 mA/cm^2 between 5.2 and 3.5 V.

Recently, Sun et al. reported a useful concept of ZnO coating for improving cycle performance of $LiNi_{0.5}Mn_{1.5}O_4$ at high temperature. The high temperature test was a very powerful way to present the merits of the ZnO coating for the $Li/LiNi_{0.5}Mn_{1.5}O_4$ cell. Even though this material was synthesized using a different chelating agent (glycolic acid) and at a different synthetic temperature (850 °C) [20], it exhibited similar properties compared with $LiNi_{0.5}Mn_{1.5}O_4$ obtained by the sol–gel method in this study. It still also showed the NiO impurity and a small 4.1 V plateau in the charge/discharge curves. Therefore, we assume that $LiNi_{0.5}Mn_{1.5}O_4$ by Sun et al. has a high probability to have lower nickel content, even though it presented an excellent cycle performance at room temperature. The work of Sun et al. reminded us of the difficulty of synthesizing $LiNi_{0.5}Mn_{1.5}O_4$ material and the importance of the electrolyte for 5 V lithium secondary batteries.

To investigate the difference in the characteristics of the two $LiNi_{0.5}Mn_{1.5}O_4$ materials, the morphologies of the two powders were observed using a scanning electron microscope (SEM). Figs. 4(a) and (c) show the SEM images of S-$LiNi_{0.5}Mn_{1.5}O_4$, which were taken at various magnifications. It was composed of well-crystalline homogeneous particles and the average particle size was about 1.5 μm. This shows the typical powder characteristic of $LiNi_{0.5}Mn_{1.5}O_4$ obtained using the sol–gel method. Meanwhile, the C-$LiNi_{0.5}Mn_{1.5}O_4$ (Fig. 4(b)) showed a slightly increased particle size (Av. 3.5 μm) and the crystalline shape is considerably different compared to that of the $LiNi_{0.5}Mn_{1.5}O_4$ powders obtained by the sol–gel method. However, Fig. 4(d) suggested one more interesting fact to us, i.e., the particle shape of $LiNi_{0.5}Mn_{1.5}O_4$ obtained by the composite carbonate process did not appear as a single particle like that from the solid-state method. Although the majority of particle shapes were about 3–4 μm sphere type at a lower magnification (5000×), the SEM image at higher magnification (50 000×) revealed that the surface of the powder was an aggregate of many small particles. Each large particle was composed of these small nano-sized particles about 50–100 nm. Furthermore, the real primary particle size of this material was 10 times smaller than that of $LiNi_{0.5}Mn_{1.5}O_4$ obtained by the sol–gel method. These nano-sized particles improved the structural stability of $LiNi_{0.5}Mn_{1.5}O_4$ powders during lithium insertion/extraction in the high voltage region.

Additionally, we suggest that the composite carbonate process has two advantages when synthesizing the $LiM_xMn_{2-x}O_4$-based materials (M: doped metal ions). First, the wide doping range of the transitional metal ions. When $LiM_xMn_{2-x}O_4$ was synthesized by the solid-state reaction or sol–gel method, it often showed the limit of substitution in the spinel structure. Sometimes, it failed to form a solid solution with the parent material or resulted in serious problems with respect to the

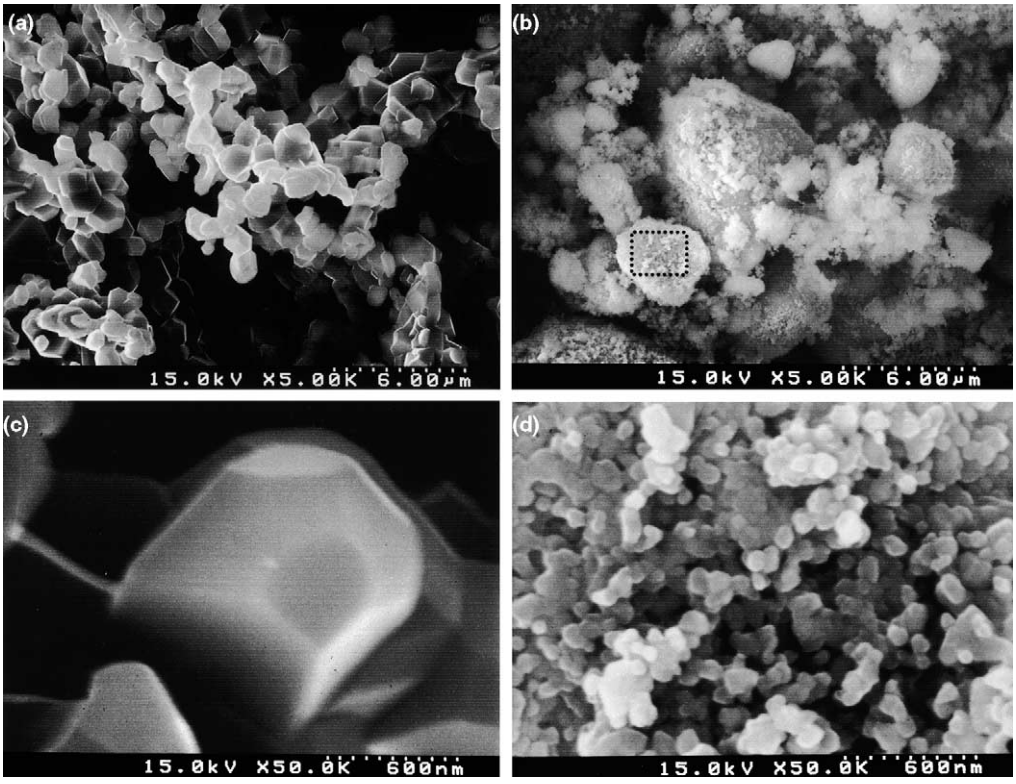

Fig. 4. Scanning electron microscope images of $LiNi_{0.5}Mn_{1.5}O_4$ obtained by the sol–gel method (a, c) and composite carbonate process (b, d).

characteristics of the synthesized materials. In the composite carbonate process, because the (M + Mn) sediment was previously formed by the reaction with $(NH_4)_2CO_3$, it was possible to make a precursor in a stoichiometric molar ratio without the lithium content or other effects. Therefore, it could be easily synthesized as the estimated resulting compound, regardless of the amount of doped metal ions. Second, the easy control of the particle size and surface area of the resulting powder. It is well known that the specific surface area is an important factor to stabilize the performance of lithium secondary batteries. When lithium and the pre-calcined (M + Mn) precursors were calcined in the furnace, the nano-sized particles were agglomerated into large micro-sized particles by continuous calcination. Although there was a high possibility that a significantly increased surface area of C-$LiNi_{0.5}Mn_{1.5}O_4$ would result in the collapse of the structure due to an excess reaction between the very small nano-particles and electrolyte, well-optimized synthetic conditions using the composite carbonate process could maintain the most favorable powder properties of C-$LiNi_{0.5}Mn_{1.5}O_4$, which existed in the form of agglomeration, for the 5 V cathode material. Actually, even though C-$LiNi_{0.5}Mn_{1.5}O_4$ had 10 times smaller primary particle size, the surface area of it was only four times greater than that of S-$LiNi_{0.5}Mn_{1.5}O_4$ as shown in Table 1. Therefore, we found that the average particle size and surface area of the resulting powder could be controlled during the synthesis and calcination processes. These were several reasons, which gave a new view of the composite carbonate process.

From these results, we concluded that $LiNi_{0.5}Mn_{1.5}O_4$ synthesized by the composite carbonate process had the desired stoichiometric nickel content, a small nano-sized particle, and well-optimized surface area during the synthetic process. These three characteristics were the main reasons that improved the cycling performance of the $LiNi_{0.5}Mn_{1.5}O_4$ material at both room and high temperatures.

4. Conclusion

$LiNi_{0.5}Mn_{1.5}O_4$ has been synthesized using the composite carbonate process at 700 °C in air. It had a pure cubic spinel structure without any impurities and only one 4.7 V plateau in the charge/discharge curve. Furthermore, it presented an excellent cycle performance at high temperature as well as at room temperature, in which the cycle retention rate during the high temperature test was 96%. The $LiNi_{0.5}Mn_{1.5}O_4$ obtained by the composite carbonate process was formed from many 3–4 μm spherical particle, which were composed of nano-sized small particles (50–100 nm). The small particle sizes and perfectly substituted nickel ions in the $LiMn_2O_4$ structure improved the cycling performance of $LiNi_{0.5}Mn_{1.5}O_4$ in the 5 V region.

References

[1] J.M. Tarascon, E. Wang, F.K. Shokoohi, W.R. Mckinnon, S. Colson, J. Electrochem. Soc. 138 (1995) 2859.
[2] L. Guohua, H. Ikuta, T. Uchida, M. Wakihara, J. Electrochem. Soc. 143 (1996) 178.
[3] Z. Lu, D.D. MacNeil, J. Dahn, Electrochem. Solid-State Lett. 4 (11) (2001) A191.
[4] T. Ohzuku, K. Nakura, T. Aoki, Electrochem. Acta 45 (1999) 151.
[5] C. Delmas, Mater. Sci. Eng. B 3 (1989) 97.
[6] C. Sigala, D. Guyomard, Solid State Ionics 81 (1995) 167.
[7] Q. Zhong, A. Bonakdarpour, M. Zhang, Y. Gao, J.R. Dahn, J. Electrochem. Soc. 144 (1997) 205.
[8] K. Amine, H. Tukamoto, H. Yasuda, Y. Fujita, J. Power Sources 68 (1997) 604.
[9] J.B. Bates, D. Lubben, N.J. Dudney, F.X. Hart, J. Electrochem. Soc. 142 (1995) L149.
[10] M.M. Thackeray, J. Electrochem. Soc. 144 (1995) L100.
[11] Y. Todorov, C. Wang, M. Yoshio, J. Int. Meeting Electrochem. Soc. Ins. Soc. Electrochem. (1997) 31.
[12] Y. Ein-Eli, W.F. Howard Jr., J. Electrochem. Soc. 144 (1997) L205.
[13] H. Kawai, M. Nagata, H. Tukamoto, A.R. West, Electrochem. Solid-State Lett. 1 (5) (1998) 212.
[14] H. Narai, Y. Idemoto, N. Koura, The 42th Battery Symposium in Japan, Yokohama, 21–23 November 2001; Meeting Abstract (2001) 140.
[15] Y.S. Lee, Y.K. Sun, K.S. Nahm, Solid State Ionics 109 (1998) 285.
[16] Y.K. Sun, Y.S. Jeon, H.J. Lee, Electrochem. Solid-State Lett. 3 (1) (2000) 7.
[17] Y.S. Lee, Y.M. Todorov, T. Konishi, M. Yoshio, ITE Lett. Batteries New Technol. Med. 1 (2000) 883.
[18] R. Alcantara, M. Jaraba, P. Lavela, J.L. Tirado, Electrochem. Acta 47 (2002) 1829.
[19] K. Amine, H. Tukamoto, H. Yasuda, Y. Fujita, The Electrochemical Society Meeting Abstract, Chicago, PV 95-2 (1995) 114.
[20] Y.K. Sun, Y.S. Lee, M. Yoshio, K. Amine, Electrochem. Solid-State Lett. 5 (5) (2002) A99.